

The Thermal Phase Transition in Nuclear Multifragmentation: The Role of Coulomb Energy and Finite Size

B. K. Srivastava¹, S. Albergo², F. Bieser⁶, F. P. Brady³, Z. Caccia², D. A. Cebra³, A. D. Chacon⁷, J. L. Chance³, Y. Choi¹, S. Costa², J. B. Elliott¹, M. L. Gilkes¹, J. A. Hauger¹, A. S. Hirsch¹, E. L. Hjort¹, A. Insolia², M. Justice⁵, D. Keane⁵, J. C. Kintner³, V. Lindenstruth⁴, M. A. Lisa⁶, H. S. Matis⁶, M. McMahan⁶, C. McParland⁶, W. F. J. Müller⁴, D. L. Olson⁶, M. D. Partlan³, N. T. Porile¹, R. Potenza², G. Rai⁶, J. Rasmussen⁶, H. G. Ritter⁶, J. Romanski², J. L. Romero³, G. V. Russo², H. Sann⁴, R. P. Scharenberg¹, A. Scott⁵, Y. Shao⁵, T. J. M. Symons⁶, M. Tincknell¹, C. Tuvé², S. Wang⁵, P. Warren¹, H. H. Wieman⁶, T. Wienold⁶, and K. Wolf⁷

(EOS Collaboration)

¹*Purdue University, West Lafayette, IN 47907*

²*Università di Catania and Istituto Nazionale di Fisica Nucleare-Sezione di Catania,
95129 Catania, Italy*

³*University of California, Davis, CA 95616*

⁴*GSI, D-64220 Darmstadt, Germany*

⁵*Kent State University, Kent, OH 44242*

⁶*Nuclear Science Division, Lawrence Berkeley National Laboratory, Berkeley, CA 94720*

⁷*Texas A&M University, College Station, TX 77843*

(November 12, 2018)

A systematic analysis of the moments of the fragment size distribution has been carried out for the multifragmentation (MF) of 1A GeV Au, La, and Kr on carbon. The breakup of Au and La is consistent with a continuous thermal phase transition. The data indicate that the excitation energy per nucleon and isotopic temperature at the critical point decrease with increasing system size. This trend is attributed primarily to the increasing Coulomb energy with finite size effects playing a smaller role.

PACS number: 25.70Pq; 05.70.Jk

The EOS collaboration has recently studied the multifragmentation (MF) of 1A GeV Au on carbon [1–10]. One of the important results was the possible observation of critical behavior and the extraction of associated critical exponents [1,3,5]. The values of these exponents were very close to those of ordinary fluids indicating that MF may arise from a continuous phase transition and may belong to the same universality class as ordinary fluids. Another important result was the successful description of the EOS MF data by statistical thermodynamical models, which describe quantum mechanically the MF of a charged nucleus [10–15]. In this paper we analyze the recent results for MF of 1AGeV La and Kr on C [8] along with those previously reported for Au [1,3,5] in the manner proposed by Campi [16–18]. Our analysis provides the first experimental evidence for the evolution of the MF mechanism with increasing projectile size and for the effects of Coulomb energy and finite size.

The reverse kinematics experiments and the analysis by which the equilibrated remnant, which undergoes MF, was separated from promptly emitted particles and the details of the determination of the remnant mass and excitation energy are given in our earlier publications [2,4,8].

Campi [16–18] and Bauer [19,20] first suggested that the methods used in percolation studies may be applied to MF data. In percolation theory the moments of the cluster distribution contain the signature of critical behavior [21]. The method of moments analysis was used by several groups [22–25] to search for evidence of the liquid-gas phase transition in MF. Thus for each event, we determine the total multiplicity of charged fragments, m , and the number of charged fragments n_A , of nuclear charge Z and mass A [2]. We calculate the k moments of the cluster size distribution given by

$$M_k(m) = \sum A^k n_A(m) \quad (1)$$

where the sum runs over all masses in the event including neutrons except for the heaviest fragment. This quantity was instrumental in extracting the critical exponents in Au+C data

[1]. It has been argued that there should be an enhancement in the critical region of the moments, M_k , for $k > \tau - 1$, with critical exponent $\tau > 2$ [16,17]. For example, the reduced variance γ_2 , i.e. the combination of moments given by

$$\gamma_2 = M_2 M_0 / M_1^2 \quad (2)$$

has a peak value of 2 for a pure exponential distribution, $n_A \sim e^{-\alpha A}$, regardless of the value of α , but $\gamma_2 > 2$ for a power law distribution, $n_A \sim A^{-\tau}$, provided the system is large enough. Here M_1 and M_2 are the first and second moments of the mass distribution in an event and M_0 is the total multiplicity including neutrons.

FIGURES

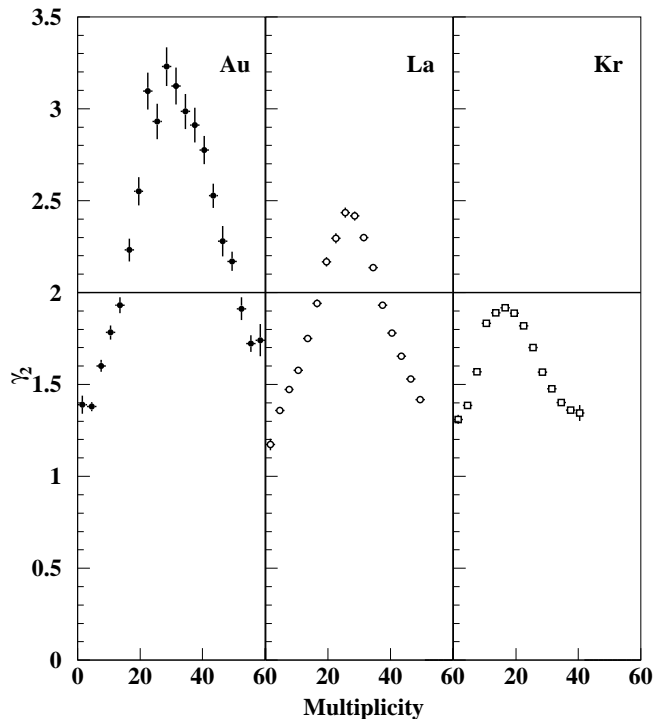


FIG. 1. γ_2 as a function of multiplicity from Au, La, and Kr systems

We have calculated γ_2 event by event as a function of total charged particle multiplicity for all three systems, as shown in Fig.1. It is clear that for Au and La $\gamma_2 > 2$ at the peak, while for Kr $\gamma_2 < 2$. The position of the maximum γ_2 value defines the critical point, m_c , where the fluctuations in the fragment sizes are the largest. To obtain m_c accurately for each system a high resolution version of Fig.1, with points corresponding to each value of m , was fitted with a polynomial of order 3-9 and the fit with the best chi-square per degree of freedom was then chosen to locate the multiplicity at which γ_2 reaches a maximum. The decrease in γ_2 with decrease in system size observed in Fig.1 is also seen in 3d percolation studies and has been attributed to finite size effects [18].

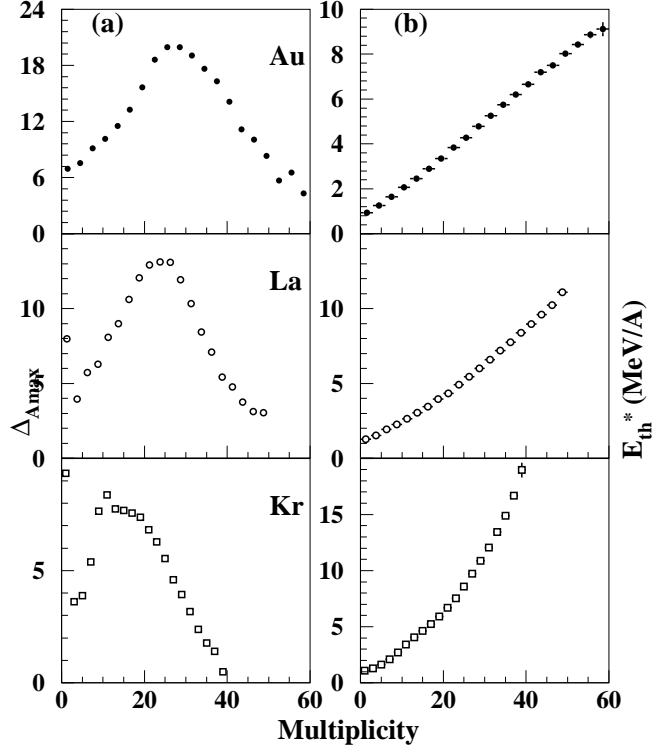


FIG. 2. a).Fluctuations in the size of the largest fragment as a function of multiplicity. b).Excitation energy as a function of multiplicity.

Another way of identifying the critical point is from the fluctuations in the size of the largest fragment. The fluctuations in this quantity, Δ_{Amax} , peak at the critical point as shown in Fig.2(a). For Kr the peak in Δ_{Amax} is not as well defined as for Au and La. One sees a peak in Δ_{Amax} for Kr at $m \sim 10$. This corresponds to ~ 3 MeV/nucleon excitation energy, which is too low for MF to occur. Thus in case of Kr the m_c value was obtained from Fig.1 only. For Au and La m_c was obtained as the average of the two peak values in Figs.1 and 2. The m_c values for Au, La, and Kr are 28 ± 3 , 24 ± 3 , and 18 ± 2 , respectively. The m_c value for Au is in agreement with our earlier reported values for Au within the respective uncertainties [1,5].

The thermal excitation energy, E_{th}^* , i.e. the energy available for particle and fragment emission, is a more fundamental quantity than the multiplicity. The experimental relation between these two quantities [8] is shown in Fig.2(b).

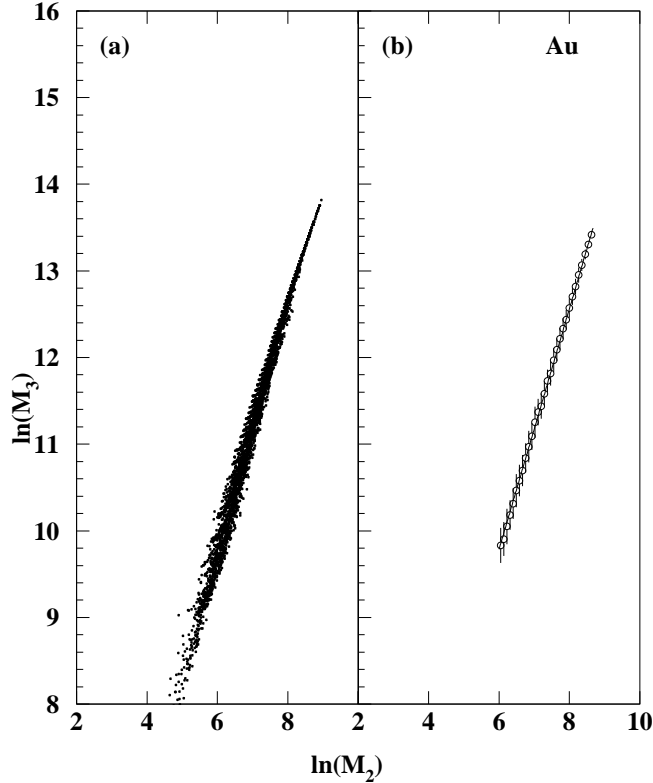


FIG. 3. a). $\ln(M_3)$ vs $\ln(M_2)$ for Au above the critical multiplicity. b). The average value of $\ln(M_3)$ at a given $\ln(M_2)$.

To extract the power law exponent τ , we examine the MF region above m_c , i.e. the region past the peak in Fig.1 [26]. Fig.3(a) shows a scatter plot of $\ln(M_3)$ vs $\ln(M_2)$ for Au [1,16,22]. The slope, S , of the line through the points is related to the exponent τ , $S = (\tau - 4) / (\tau - 3)$. To obtain τ we plot the average value of $\ln(M_3)$ vs $\ln(M_2)$, Fig.3(b). We fit the region between $E_{th}^* = 5.5 - 7.5$ MeV/nucleon to obtain the τ value. The lower energy is ~ 1 MeV/nucleon higher than the energy corresponding to the peak in γ_2 and the higher value is close to the end of γ_2 branch above m_c in Fig.1. We obtain $\tau = 2.16 \pm 0.08$ for Au with χ^2/dof of 1. This value is in agreement with the τ value from the single parameter fit, $n_A = q_0 A^{-\tau}$, at m_c [5,21]. The same procedure was followed to fit $\ln(M_3)$ vs $\ln(M_2)$ for La as shown in Fig.4(b), derived from the scatter plot for La in Fig.4(a). For La we obtain $\tau = 2.10 \pm 0.06$, with $\chi^2/dof \sim 6$, again in agreement with the value obtained from the one-parameter fit at m_c .

The data for Kr are shown in Fig.5(a). There is a distinct difference between Fig.3(a),

Fig.4(a) and Fig.5(a). In the plot for Au, $\ln(M_3)$ and $\ln(M_2)$ lie on a very narrow band while for Kr there is a large variation. This difference reflects a wider fragment mass distribution for different events with the same multiplicity for Kr. A similar trend with system size is seen in percolation indicating that this is a finite size effect [26]. Fig.5(b) shows the fit for Kr. A nonlinear behavior is clearly observed. This contrasts with the linear behavior seen in the corresponding plots for Au and La in Figs.3(b) and 4(b) respectively. An exponential fit to the data is shown in Fig.5(b) to guide the eye. The fitting region was chosen by the criteria laid down in case of Au and La. A linear fit to the Kr data gives a value of $\tau = 1.88 \pm 0.08$ with an unacceptably large χ^2/dof of 20. This result is consistent with Fig.1, in which the peak γ_2 value is < 2 for Kr.

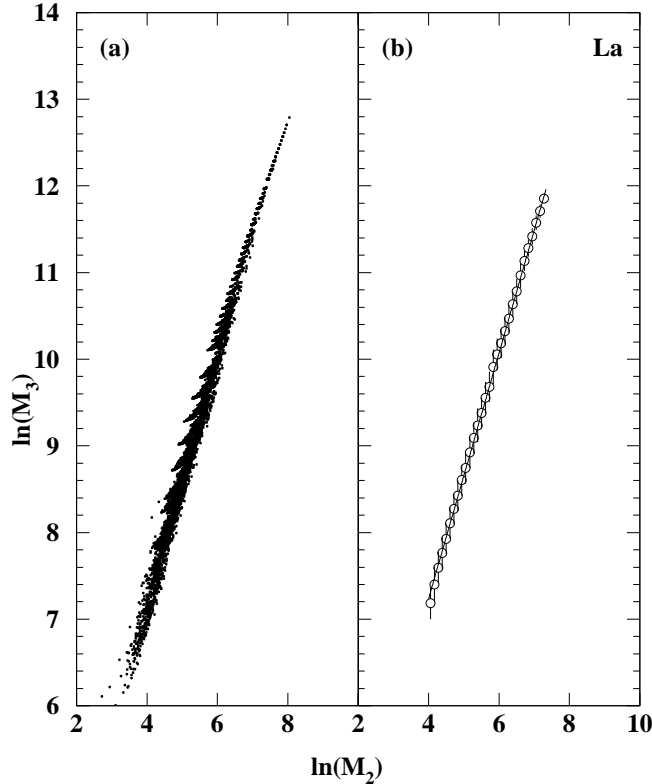


FIG. 4. a). $\ln(M_3)$ vs $\ln(M_2)$ for La above the critical multiplicity. b). The average value of $\ln(M_3)$ at a given $\ln(M_2)$.

The thermal excitation energy per nucleon at m_c , E_c^* , was obtained for each system from the variation of E_{th}^* with m as shown in Fig.2(b). The dependence of E_c^* on system size is shown in Fig.6(a), where the size of fragmenting system is the average remnant mass at m_c

[8]. The width of the remnant mass distribution at m_c is indicated by the horizontal error bars and is $\sim 6-8\%$ [4,8]. Fig.6(b) shows the isotope freeze-out temperature, T_{He-DT} , obtained from the H^2/H^3 and He^3/He^4 double isotope ratios at m_c [8,27]. Both E_c^* and T_{He-DT} decrease with increasing system size. We can compare these results with calculations which have studied highly excited nuclear matter. The temperature-dependent Hartree-Fock(HF) calculations for equilibrated hot nuclei show that Coulomb repulsion causes the compound nucleus to become unstable at a lower temperature than the uncharged system [28]. The trend seen in the present work is also seen in a HF calculation using a Skyrme interaction with a soft equation of state [29]. This temperature is shown in Fig.6(b) as T_{limit} . In another study [30] it was found that finite size effects and Coulomb force lead to a considerable reduction in the “critical” temperature.

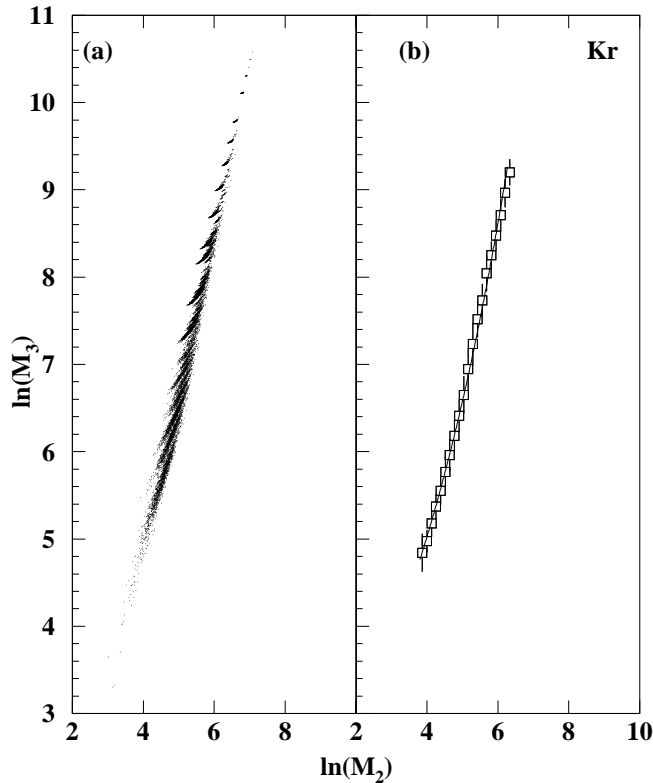


FIG. 5. (a). $\ln(M_3)$ vs $\ln(M_2)$ for Kr above the critical multiplicity. (b). Average $\ln(M_3)$ as a function of $\ln(M_2)$.

The Au, La and Kr results can also be compared with the statistical multifragmentation model (SMM) [10,11]. The SMM E_c^* values are shown in Fig.6(a). The agreement between

data and SMM is good although a ~ 1 MeV/A discrepancy is observed for Kr. The SMM breakup temperature T_{SMM} [11] is shown in Fig.6(b). There is a decrease in both temperatures with increasing system size. It is apparent that the T_{He-DT} temperature is about 1 MeV lower than the SMM temperature. This difference is due to the fact that T_{He-DT} is measured after secondary decay has taken place, while T_{SMM} corresponds to the breakup configuration. Particularly interesting is the fact that the experimental T_{He-DT} tracks T_{SMM} in its dependence on system size at m_c . SMM indicates that the decrease in both T_{SMM} and in E_c^* with increasing system size is due to the increase of the Coulomb energy. This result suggests that the Coulomb energy plays a central role in the MF of nuclei.

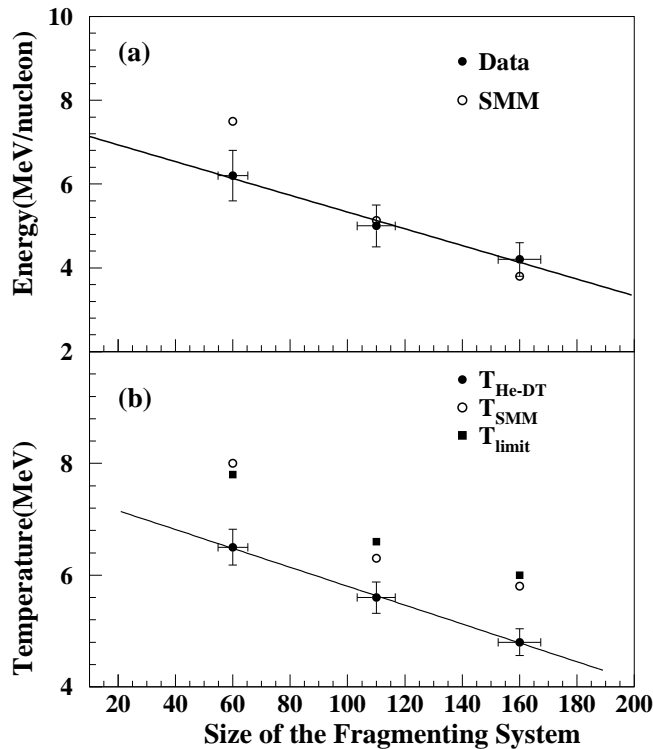


FIG. 6. a). Energy (MeV/nucleon) at $m = m_c$. b). T_{He-DT} , T_{SMM} and T_{limit} as a function of the system size. The lines through the points are linear fits to the data.

The microcanonical Metropolis Monte Carlo (MMMC) [12,13] calculations have emphasized that MF is controlled by the competition between long range Coulomb forces and finite size effects. Finite size effects in models with only short range forces predict an *increase* in the critical temperature as the system size increases, as is evident from percolation [31] and

Ising model studies [32]. Since the experimental temperature exhibits the opposite dependence on system size, it is apparent that Coulomb effects are more important than finite size effects. For finite *neutral* matter the critical temperature (T_c) is expected to be ~ 15 - 20 MeV [30,33]. The observed T_c for $A=160$ is ~ 6 MeV. Compared to finite uncharged nuclei, the presence of Coulomb energy plays a role in lowering the excitation energy needed to reach the regime where critical signatures are observed. In the smaller Kr system there is less Coulomb energy in the initial remnant state. Achieving multifragmentation in this system requires greater excitation energy/nucleon compared to Au and La (as shown in Fig.6) and as a result, the dynamics of the ensuing disassembly may not take this system near its critical regime.

In conclusion, we have analyzed the fragment distributions resulting from 1A GeV Au, La, and Kr on carbon. The reduced variance γ_2 has a peak at the multiplicity where the fluctuations in A_{max} are largest. The peak value of γ_2 is > 2 for Au and La and they exhibit a power law fragment yield distribution at m_c . The peak value for Kr is < 2 and this system does not exhibit a power law with $\tau \geq 2$. The decrease in γ_2 with decreasing system size can be attributed to finite size effects. These observations argue against a continuous phase transition in the MF of Kr but are consistent with such a transition in the MF of La and Au. Recent analysis based on the SMM microcanonical caloric curve [10], which indicated a first order phase transition for the MF of Kr and a continuous phase transition for the MF of Au is consistent with experimental observations. The observed decrease in excitation energy and temperature with an increase in system size for MF at the critical point shows the importance of the Coulomb energy in MF.

This work was supported by the U. S. Department of Energy.

REFERENCES

- [1] M. L. Gilkes *et al.*, Phys. Rev. Lett. 73, 1590 (1994).
- [2] J. A. Hauger *et al.*, Phys. Rev. Lett. 77, 235 (1996).
- [3] J. B. Elliott *et al.*, Phys. Lett. B381, 35 (1996).
- [4] J. A. Hauger *et al.*, Phys. Rev. C57, 764 (1998).
- [5] J. B. Elliott *et al.*, Phys. Lett. B418, 34 (1998).
- [6] J. Lauret *et al.*, Phys. Rev. C57, R1051 (1998).
- [7] B. K. Srivastava *et al.*, Phys. Rev. C60, 064606 (1999).
- [8] J. A. Hauger *et al.*, Phys. Rev. C62 024616 (2000).
- [9] J. B. Elliott *et al.*, submitted to Phys. Rev. C
- [10] R. P. Scharenberg *et al.*, submitted to Phys. Rev. C
- [11] J. Bondorf *et al.*, Phys. Rep. 257, 133 (1995).
- [12] D. H. E. Gross ,Rep. Prog. Phys. 53, 605 (1990).
- [13] D. H. E. Gross , Phys. Rep. 279, 119(1997).
- [14] R. P. Scharenberg, Proceedings of the International Workshop XXVII on Gross Properties of Nuclei and Nuclear Excitations, Hirschegg, Austria, p 237 , GSI 1999.
- [15] B. K. Srivastava, Proceedings of the International Workshop XXVII on Gross Properties of Nuclei and Nuclear Excitations, Hirschegg, Austria, p 247 , GSI 1999.
- [16] X. Campi, J. Phys. A 19, L917, (1986).
- [17] X. Campi, Phys. Lett. B 208, 351, (1988).
- [18] X. Campi, Proceedings of the International School of Physics 'Enrico Fermi' Nuclear Collisions from the Mean-Field into the Fragmentation regime, CXII 331, (1991).

- [19] W. Bauer *et al.*, Phys. Lett. B150, 53 (1985).
- [20] W. Bauer *et al.*, Nucl. Phys. A452, 699 (1986).
- [21] D. Stauffer and A. Aharony, Introduction to Percolation Theory (Taylor and Francis , London, 1992).
- [22] W. Bauer, Phys. Rev. C38, 1297(1988).
- [23] P. Kreuzt *et al.*, Nucl. Phys. A556, 672 (1993).
- [24] M. Belkacem *et al.*, Phys. Rev. C54, 2435 (1996).
- [25] P. F. Mastinu *et al.*, Phys. Rev. C57, 831, (1998).
- [26] J. B. Elliott *et al.*, Phys. Rev. C49, 3185 (1994).
- [27] S. Albergo *et al.*, Nuovo Cimento A89, 1(1985).
- [28] P. Bonche *et al.*, Nucl. Phys. A436, 265 (1985).
- [29] S. Levit and P. Bonche , Nucl. Phys. A437, 426 (1985).
- [30] H. R. Jaqaman *et al.*, Phys. Rev. C29, 2067 (1984).
- [31] D. W. Heerman and D. Stauffer , Z. Phys.B44, 339 (1981).
- [32] J. M. Carmona *et al.*, Nucl Phys. A643, 115 (1998).
- [33] J. M. Lattimer *et al.*, Nucl. Phys. A432, 646 (1985).